

Hybrid railway power quality conditioner for high-capacity traction substation with auto-tuned DC-link controller

Adel Tabakhpour Langerudy , Sayed Mohammad Mousavi G

Department of Railway Electrification, Iran University of Science and Technology, Narmak, Tehran 16846-13114, Iran

 E-mail: tabakhpour@gmail.com

ISSN 2042-9738

Received on 3rd November 2015

Revised on 26th December 2015

Accepted on 3rd February 2016

doi: 10.1049/iet-est.2015.0045

www.ietdl.org

Abstract: Power quality was always a major concern in designing an electric supply system for railways. Since electric railcars are usually single-phase loads, they draw high amounts of negative sequence component of currents, in addition to harmonic contents and transient currents. Therefore, many compensation methods were examined to improve the power quality indices. The active power quality conditioner (APQC) can be considered as an ideal compensator for high-speed railway, which contains a three-phase converter connected to the traction substation through a step-down transformer. However, with the growth of railway loads, the nominal rating of the solid-state high-frequency switches of APQC increases seriously, which in turn, results in an exponential growth of the cost of power-electronic switches. Therefore, for a very high-capacity railway system, it is not economic to apply an APQC. As a solution, a combination of APQC with the static VAR compensator is proposed in this study, which reduces the rating of APQC, and improves the power quality of the system. Simulation results validate the pre-defined hypothesis. Moreover, the performance of APQC depends on the DC-link operation, for which genetic-algorithm optimisation has been applied to obtain an optimum design of a stable DC-link voltage.

1 Introduction

Railway electrification has begun in the early 20th century. It was embraced in many countries because of many advantages, e.g. lower air pollution, heavy load and mass transit ability, high efficiency, and reduced CO₂ generation [1, 2]. From the start of railway electrification, power quality was a significant concern for electrification apologists, and many research studies have been dedicated to power quality improvement in electrical railway distribution systems. Early approaches to power quality improvement were mainly simple solutions; for instance, three-phase trains [3], phase-shift method, and later on, use of balanced transformers [4]. However, these approaches could solve the power quality problems only when the traction sections are loaded fully and equally. In order to improve the power quality dynamically, static VAR compensators (SVCs) were applied at railway systems, to compensate the unbalanced currents. The basic application of SVC is to compensate reactive power in the distribution system. In the railway systems, the main problem is, however, unbalanced currents due to single-phase trains. Therefore, control strategy of SVC was adopted to compensate unbalanced currents based on Steinmetz law [5], which is explained in the next section. SVC can compensate the unbalanced currents in every loading condition; however, harmonic currents remain as a major problem for system. In addition, adopting SVC has a negative effect on resonance frequency of the system [6, 7].

The railway static power conditioner (RPC) was introduced to compensate all the three major concerns of power quality in railway systems [8], which are unbalanced currents, harmonic contents of currents, and reactive power. RPC contains two back-to-back single-phase converters sharing a same DC-link capacitor, which transfers active and reactive powers between the two sections, compensating the harmonic currents, simultaneously. Active power quality conditioner (APQC) is the next generation of RPC, which includes a three-phase converter, introduced in [9, 10]. It does the same operation as RPC, saving two power-electronic switches, without increasing the rating of switches, which is described in the next section in detail. The

APQC can be an ideal compensator to improve the power quality of a railway system; however, it uses expensive power-electronic switches, resulting in very high costs. Moreover, applying the APQC becomes more and more expensive with the increasing capacity of traction substations (TSSs). For higher rates of power switches, the cost of APQC would increase exponentially, which makes it impossible for high-capacity TSSs.

In this paper, a combination of APQC and SVC is proposed as an alternative, which solves the economic problem of APQC, and improves the total performance of the compensator. In this combination scheme, compensating the negative sequence component (NSC) of currents is devolved to the SVC, and the rest of currents are sensed by the APQC, resulting in reduced rating of power-electronic switches. It will, in turn, result in lower cost of the total compensator, for heavy high-speed railway systems.

2 Description of the railway system with SVC and APQC

2.1 Railway system

For high-speed railway, V–v transformers are usually used in TSSs due to their high utilisation factor [9] (i.e. 100% for a fully compensated load). In the secondary side of TSS, one phase is connected to the return circuit (i.e. running rails), and the two other phases are connected to the two electrically-separated sections of the catenary wire, as shown in Fig. 1.

A traction load with V–v TSS draws an NSC current between half and one times the positive sequence component (PSC) [9]. Since high-speed trains are considered as heavy loads in a power plant, these high-NSC currents may have destructive effects on the entire system, e.g. producing an opposite direct torque in machines, and occupying the line capacity. Furthermore, use of power switching devices (e.g. in traction motor drives, auxiliary power supplies) and interaction of pantographs/brushes with catenary/third-rail results in arcs, harming the system operation as well. Therefore, the power quality of the electric railway system has to be

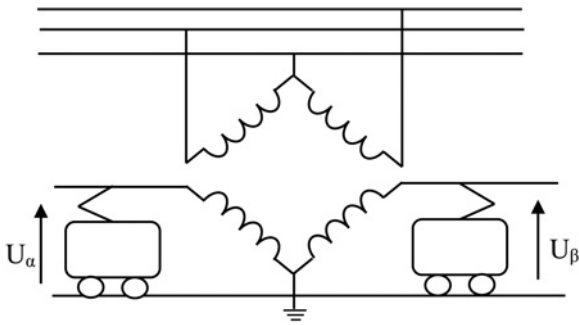


Fig. 1 V-v TSS feeding trains from a three-phase power plant

considered as a serious problem, which severely needs to be improved [4, 11].

2.2 Static VAR compensator

SVC includes three variable delta-connected impedances, used to compensate the reactive power in distribution or transmission systems. For systems with high NSC such as electric railway, control strategy of SVC can be modified to eliminate the NSC based on Steinmetz law [5, 12]. Steinmetz argued that a single-phase resistive load between *a* and *b* phases which is equal to *G*, can be symmetrised by an inductive load between *a* and *c* phases equal to $G/\sqrt{3}$, and a capacitive load between *b* and *c* phases equal to $-G/\sqrt{3}$. The control unit of SVC must be designed to adjust the variable impedances to meet the balanced currents [12].

2.3 Active power quality conditioner

In APQC, a three-phase AC-DC converter with a DC-link capacitor is connected to the secondary side of the TSS, through two single-phase step-down transformers [9, 10]. APQC senses the three-phase currents at TSS, which generates three-phase compensation currents based on instantaneous power theory, resulting in a balanced three-phase current without harmonics and reactive power. APQC is expensive because of the big power switches. The most key parameter influencing the rating of APQC is the maximum unbalanced currents throughout the system [13], which occurs when one section is at full-load and the other section has no load. The power switches of APQC must be designed for worst-case condition, which is maximum unbalanced current, to meet the requirements of the system at any loading condition. Therefore, it is reasonable to devolve the NSC compensation to SVC, leading to decrement of the power-electronic switches rating.

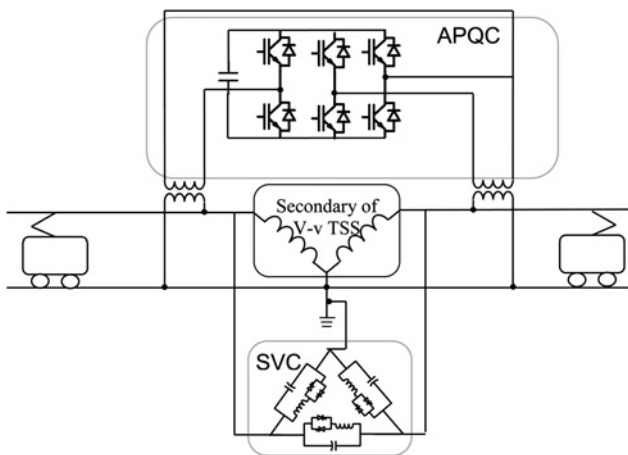


Fig. 2 Proposed HPQC installed at the secondary side of TSS

3 Modelling and control strategy of the combined SVC with APQC

APQC is employed at the secondary side of TSS, in which there could be two possible shunt combinations with the SVC: SVC can be employed at the secondary or primary sides of TSS. If it is employed at the primary side, the traditional APQC compensates all of NSC, and SVC will be useless. In this case, in order to decrease the rating of power-electronic switches, the control strategy of the APQC can be modified to compensate only harmonics and reactive power, leaving the NSC to be compensated by the SVC.

However, for the SVC at the load side, the NSC is compensated fully by the SVC, and the APQC faces only the rest of currents (i.e. the balanced currents, only including harmonics and reactive power). For this combination, the traditional control strategy of the APQC can be employed, because the sampling devices sense no unbalanced currents naturally. Furthermore, if SVC experiences a fault condition, the APQC can compensate the whole three-phase currents, resulting in increased reliability of the compensator. Therefore, hybrid power quality conditioner (HPQC) is proposed as can be seen in Fig. 2.

The compensation impedances of SVC are calculated based on Steinmetz law [5], in which the firing angles are generated by the control unit, drawn in Fig. 3. Firing angles of each two thyristors in same phases lags 180° , respect to each other. Therefore, only the signals for counterclockwise thyristors are calculated (see Fig. 2), and the signals for clockwise thyristors are calculated from their adjacent thyristors' signals with 180° delay angle.

To derive the compensation susceptances of the SVC, the NSC of current must be calculated. The objective of control is to eliminate the NSC of current; therefore, the susceptances of the SVC can be obtained, putting the NSC of current equal to zero. The compensation susceptances are expressed in (1), in which the active and reactive powers of the two sections are measured

$$\begin{pmatrix} B_{\alpha}^{\text{Comp}} \\ B_{\beta}^{\text{Comp}} \\ B_{\alpha\beta}^{\text{Comp}} \end{pmatrix} = \frac{1}{3V_L^2} \begin{pmatrix} 0 & 3 & -\sqrt{3} & 0 \\ \sqrt{3} & 0 & 0 & 3 \\ -\sqrt{3} & 0 & 0 & 3 \end{pmatrix} \begin{pmatrix} P_{\alpha} \\ Q_{\alpha} \\ P_{\beta} \\ Q_{\beta} \end{pmatrix} \quad (1)$$

In this paper, the thyristor-controlled reactor with fixed capacitors is adopted, in which the firing angles only control the inductances. To achieve the appropriate firing angles, the susceptance of fixed capacitors must be subtracted from the compensation susceptances, which results in compensation reactors, as calculated in (2)

$$\begin{pmatrix} B_{\alpha}^L \\ B_{\beta}^L \\ B_{\alpha\beta}^L \end{pmatrix} = \begin{pmatrix} B_{\alpha}^{\text{Comp}} \\ B_{\beta}^{\text{Comp}} \\ B_{\alpha\beta}^{\text{Comp}} \end{pmatrix} - \begin{pmatrix} B_{\alpha}^C \\ B_{\alpha\beta}^C \\ B_{\alpha\beta}^C \end{pmatrix} \quad (2)$$

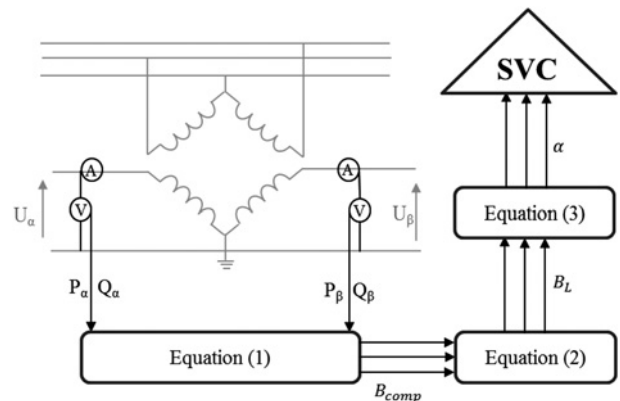


Fig. 3 Control unit of the SVC

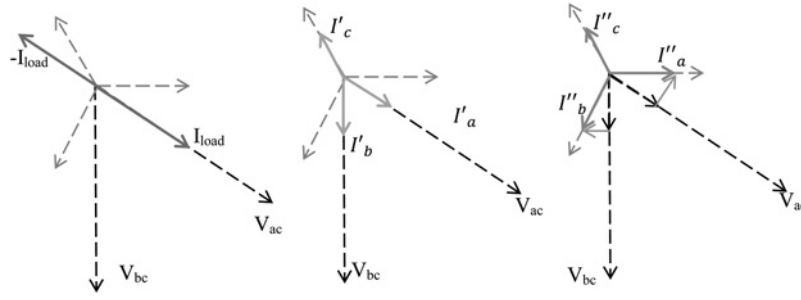


Fig. 4 Phasor diagram for compensation current calculation

Given the susceptance of the reactors, the firing angles of thyristors can be obtained by (3), as shown in Fig. 3

$$B_{\text{TCR}}^L = \frac{2\pi - 2\alpha - \sin 2\alpha}{\pi\omega L} \quad (3)$$

For the calculated firing angles, the NSC of currents equals to zero. Therefore, the control algorithms of APQC can be considered separately from SVC in this combination scheme. Accordingly, the compensation currents of APQC can be calculated for a simple V-v TSS.

The compensation currents can be calculated based on the phasor diagram, shown in Fig. 4. For clarity, the compensation currents are drawn in case of no load in left section, and full load in right section. It helps to understand the control unit designing method. Then, compensation of other loading conditions can be calculated the same as former. Totally, the compensation currents can be achieved from superposition, by adding these two compensation currents. I'_a , I'_b , and I'_c show the currents after active power balancing, and I''_a , I''_b , and I''_c denote the three-phase currents after full compensation. This method of obtaining compensation currents is based on instantaneous power theory. The voltages and currents along the line are calculated in (4)–(9)

$$\begin{pmatrix} U_\alpha \\ U_\beta \end{pmatrix} = \begin{pmatrix} \bar{V} \angle -90 \\ \bar{V} \angle -30 \end{pmatrix} \quad (4)$$

So, the currents are first calculated for no load in left section of Fig. 1. The high-speed trains use pulse width modulation drives in order to control the traction motors, which maintain the power factor near to unity [9]. Therefore, the three-phase currents can be

achieved based on the load current as in

$$\begin{pmatrix} I_a \\ I_b \\ I_c \end{pmatrix} = \begin{pmatrix} aI_{\text{Load}} \\ 0 \\ -aI_{\text{Load}} \end{pmatrix} \quad (5)$$

$$I_{\text{Load}} = \bar{I} \angle -30 \quad (6)$$

In which, a is the transformation ratio, and \bar{I} is the root-mean-square (rms) value of the train current. As shown in Fig. 2b, the currents after active power balancing is obtained, which can be written in terms of I_{Load} , as in

$$\begin{pmatrix} I'_a \\ I'_b \\ I'_c \end{pmatrix} = \begin{pmatrix} \frac{a}{2}\bar{I} \angle -30 \\ \frac{a}{2}\bar{I} \angle -90 \\ \frac{\sqrt{3}}{2}a\bar{I} \angle 120 \end{pmatrix} \quad (7)$$

The currents are not balanced yet, as seen in (7). After the reactive power balancing, as shown in Fig. 2c, the three-phase currents can be written as (8), which has no NSC and reactive power

$$\begin{pmatrix} I''_a \\ I''_b \\ I''_c \end{pmatrix} = \begin{pmatrix} \frac{a}{\sqrt{3}}\bar{I} \angle 0 \\ \frac{a}{\sqrt{3}}\bar{I} \angle -120 \\ \frac{a}{\sqrt{3}}\bar{I} \angle 120 \end{pmatrix} \quad (8)$$

Then, the left section is supposed to be at full load, while the right section has no load; in which the balanced currents can be

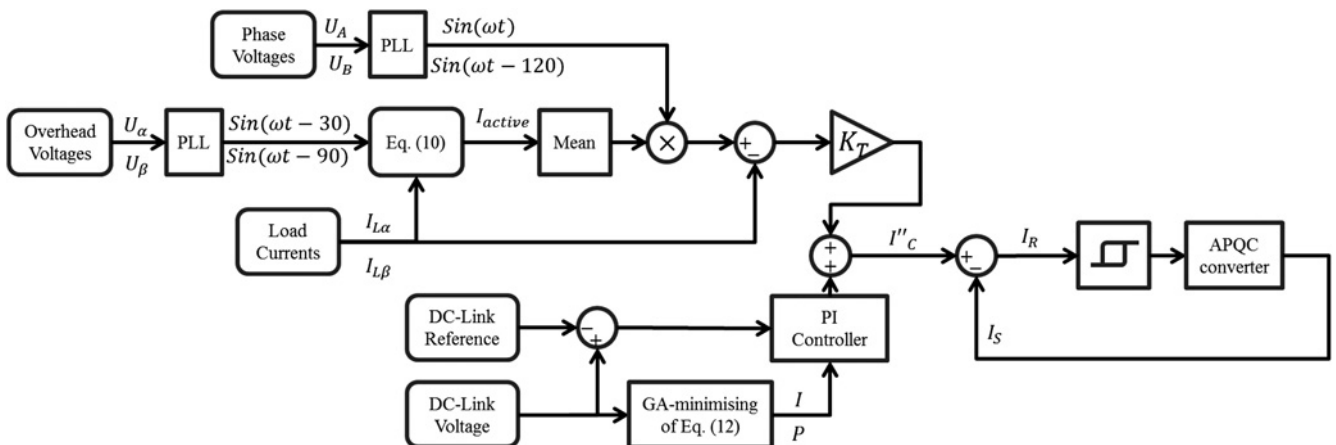


Fig. 5 Control unit of APQC, generating the pulses for IGBT gates

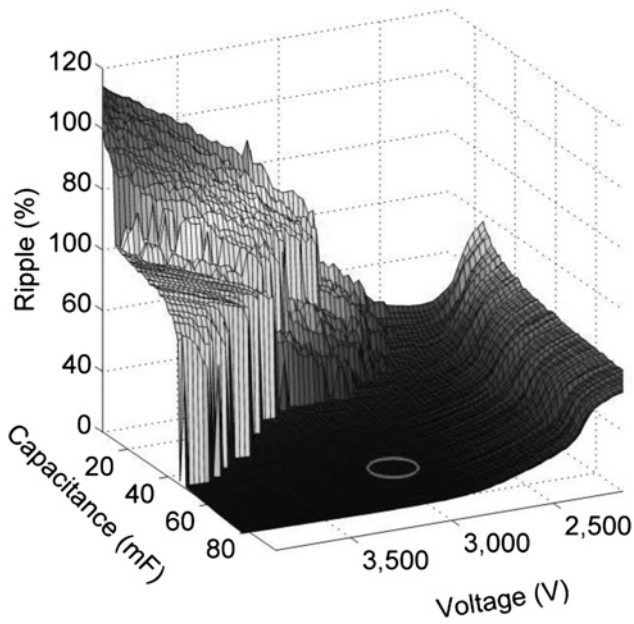


Fig. 6 Voltage ripple with respect to the DC-link voltage and capacitor

calculated. Then, the total three-phase balanced currents can be calculated based on superposition property, which results in (9)

$$\begin{pmatrix} I''_a \\ I''_b \\ I''_c \end{pmatrix} = \frac{a}{\sqrt{3}} \begin{pmatrix} (\bar{I}_\alpha + \bar{I}_\beta)\angle 0 \\ (\bar{I}_\alpha + \bar{I}_\beta)\angle 120 \\ (\bar{I}_\alpha + \bar{I}_\beta)\angle -120 \end{pmatrix} \quad (9)$$

$$|I_{\text{active}}| = \frac{2}{\sqrt{3}}(I_{L\alpha} \times \sin(\omega t - 30) + I_{L\beta} \times \sin(\omega t - 90)) \quad (10)$$

In which \bar{I}_α and \bar{I}_β are the rms values of each section's currents. Therefore, the control unit of APQC is designed to compensate the whole currents, as shown in Fig. 5, in which K_T is the transfer ratio of the two step-down single-phase transformers. The box '(10)' gives the active current as defined in (10). Consequently, the NSC is eliminated by the SVC, and the APQC only senses the harmonics and the reactive power. In addition, the performance of the APQC depends on DC-link voltage, which must be maintained constant. A PI-controller is hired to control DC-link voltage, as shown in Fig. 5.

The three-phase reference currents as calculated in (9) are compared with the three-phase currents, and the difference between them would be considered as compensation currents, as in (11). Then, a hysteresis band pulse generator is designed to generate the compensation currents which will counterbalance the total three-phase currents

$$\begin{pmatrix} I_{Ca} \\ I_{Cb} \\ I_{Cc} \end{pmatrix} = \begin{pmatrix} I_a - I''_a \\ I_b - I''_b \\ I_c - I''_c \end{pmatrix} \quad (11)$$

In which, $I_c = -(I_a + I_b)$.

4 Designing the auto-tuned DC-link parameters

In most cases, a PI-controller is hired to fix the DC-link voltage, but it should be designed precisely to achieve the quick response and low voltage ripple. In this paper, a weighted multi-objective genetic-algorithm (GA) optimisation is applied to attain the optimum parameters of the PI-controller, the DC-link voltage level, and the DC-link capacitor. The objective function is shown

Table 1 Parameters of system

line voltage	230 kV
turns ratio of TSS	230/27.5 kV
supply resistance	0.05 Ω
supply inductance	1 mH
load power (trains' total power)	6 MW
DC-link capacitor	60 mF
DC-link voltage	3 kV

Table 2 Simulation cases

case I	without compensation
case II	with APQC operation
case III	with GA-optimised APQC operation
case IV	with HPQC operation

Table 3 Loading schedule for two sections

Time	0–0.2 s	0.2–0.4 s	0.4–0.6 s
left section	full load	full load	no load
right section	no load	full load	full load

in (12), in which the ripple is defined by (13)

$$\text{O.F.} = \text{rms(ripple)} + 0.1 \times (\text{Max}(V_{DC}) - \text{Min}(V_{DC})) \quad (12)$$

$$\text{ripple} = V_{DC} - V_{\text{ref}} \quad (13)$$

GA-optimisation minimises the total difference between the measured and the desired DC-link voltage. Therefore, it leads to a quick response, because a lower difference between desired and actual DC-link voltage will result in a quicker response. Furthermore, the difference between the maximum and minimum value of DC-link voltage should be maintained in an acceptable value because of high or low voltage problems for switches, which is added to objective function with the weight of 0.1. The weight

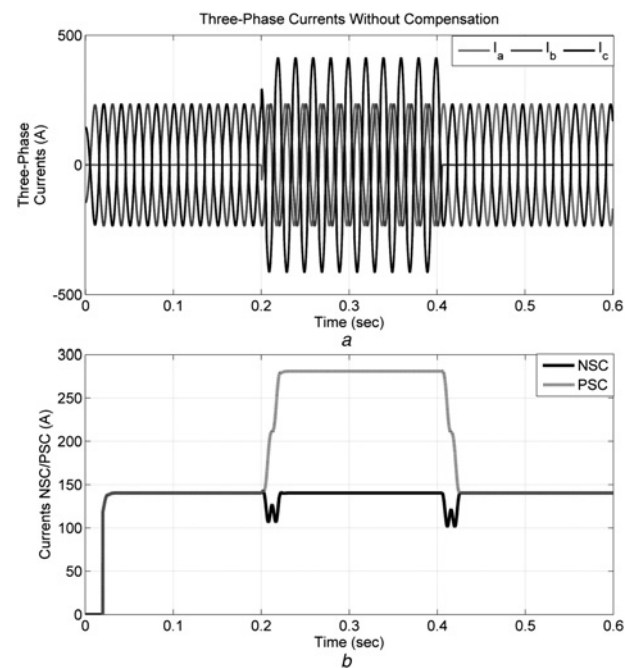


Fig. 7 Currents without compensation

a Three-phase currents
b NSC and PSC currents

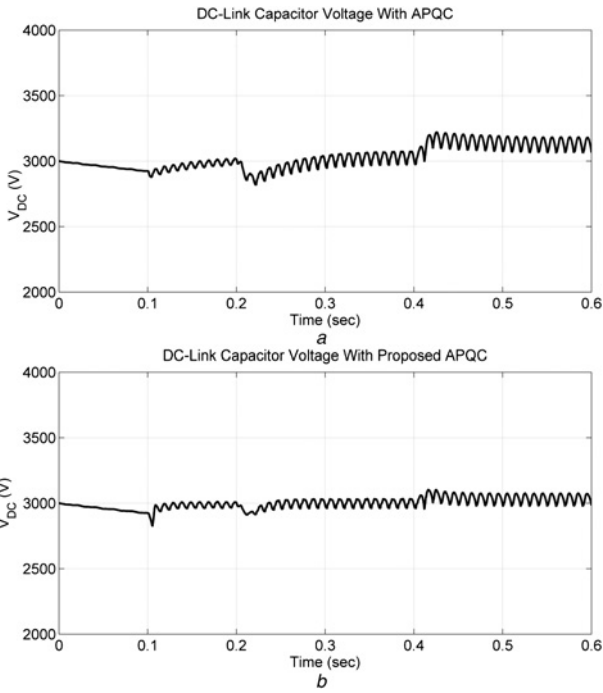


Fig. 8 DC-link voltage
 a With APQC before GA-optimisation
 b With GA-optimised APQC

0.1 is because the second term of objective function (i.e. the difference between the maximum and minimum value of DC-link voltage) is almost ten times the first term, and the function is normalised in this way. The transfer function of PI-controller is shown in (14), in which the coefficients are designed by GA

$$T_{PI} = K_p \left(1 + K_I \frac{1}{s} \right) \quad (14)$$

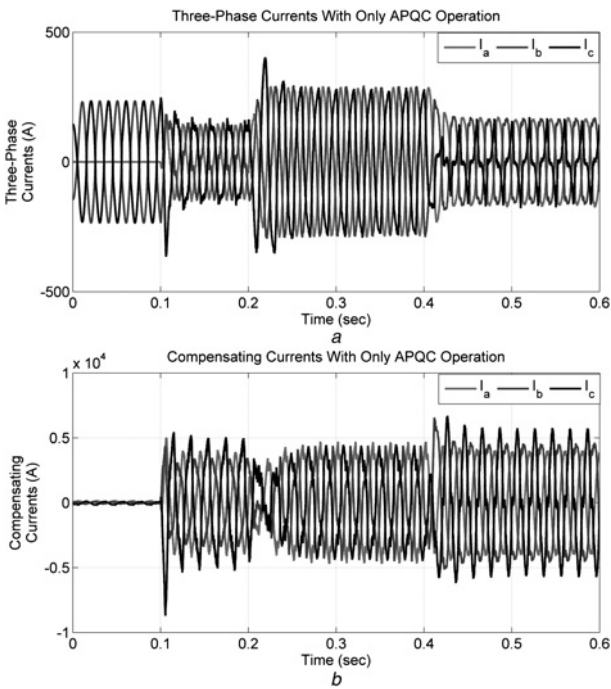


Fig. 9 GA-optimised APQC
 a Three-phase currents
 b Compensation currents

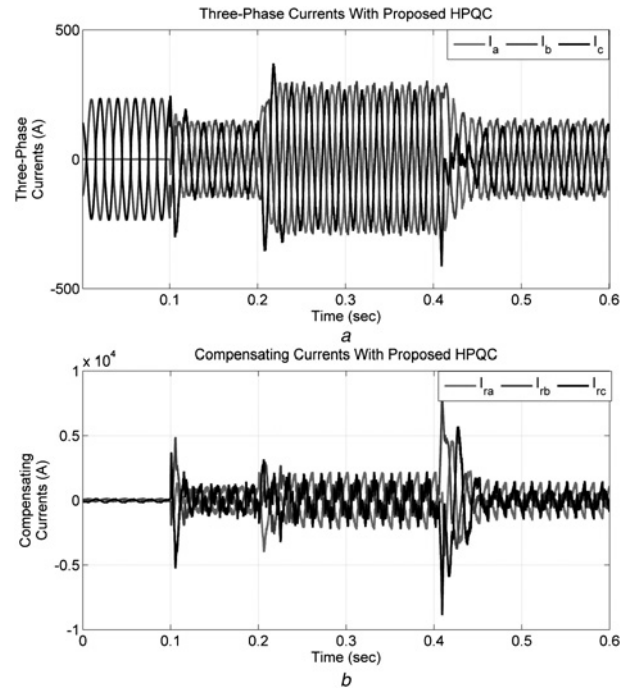


Fig. 10 HPQC operation
 a Three-phase currents
 b Compensation currents

Furthermore, the DC-link capacitor and voltage level have been selected based on the simulated DC-link voltage ripple. The capacitor and its reference voltage level have been varied in a wide range, and the voltage ripple rms has been calculated for each point, as shown in Fig. 6. As can be seen, the 3 kV and 60 mF is the first point, in which the ripple is <5%. For the higher voltages, low capacitances have very bad performances, nearly to be unstable, due to the simulation results.

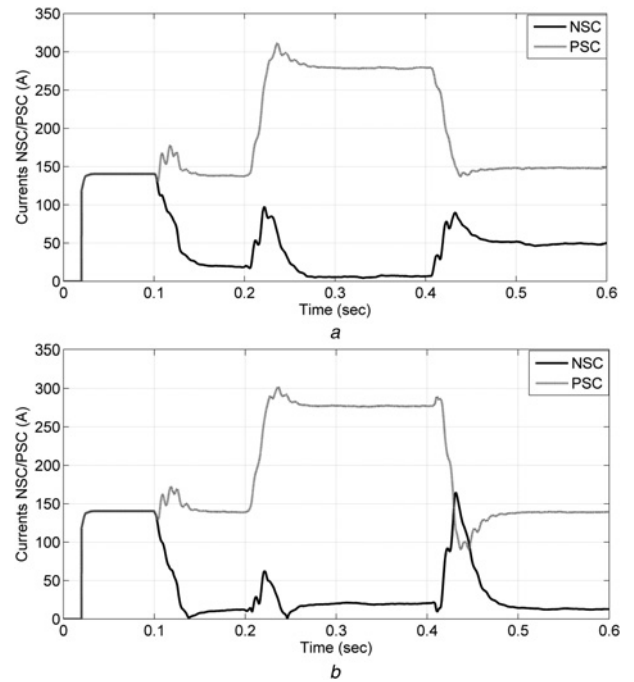


Fig. 11 NSC and PSC of three-phase current at primary side of TSS with
 a APQC operation
 b HPQC operation

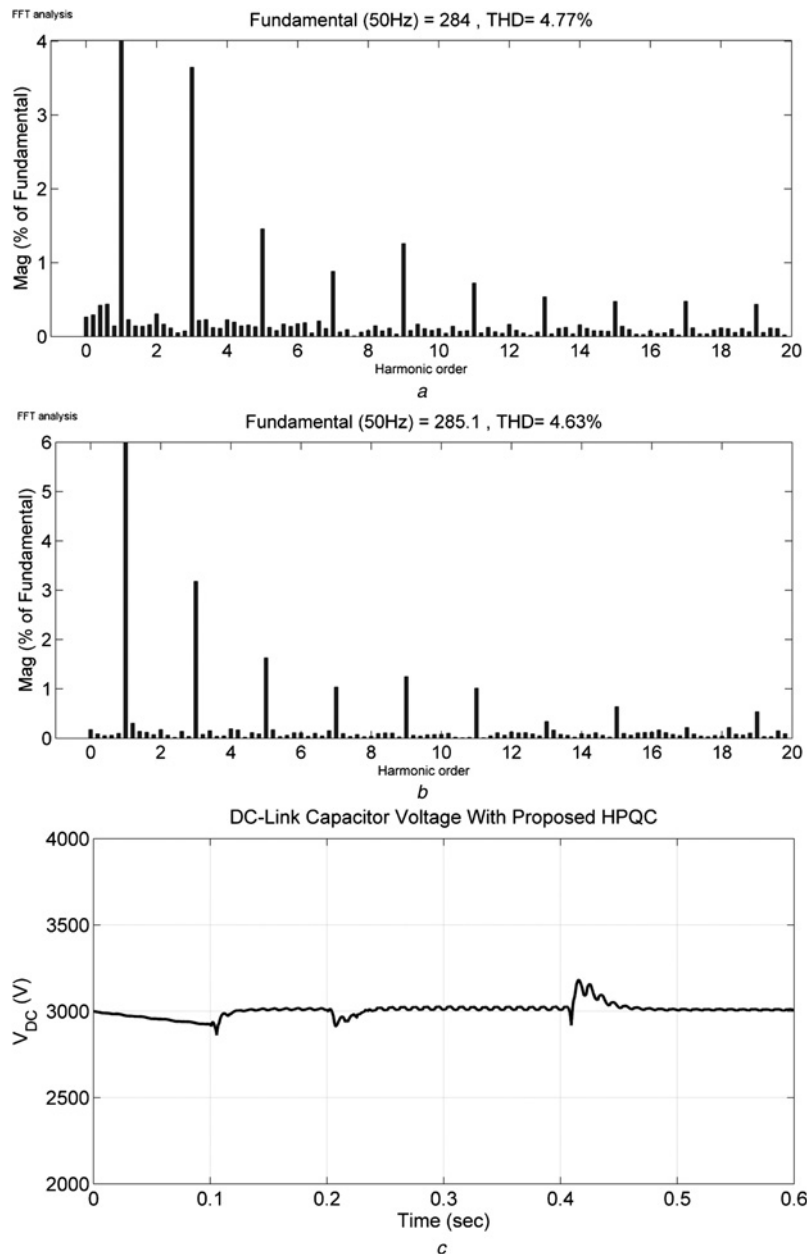


Fig. 12 Frequency domain spectrum of currents

- a For APQC
- b For HPQC
- c DC-link voltage of HPQC

The proposed GA voltage optimiser can be adopted in an online tuning processor, which maintains the P and I coefficients at the optimum values for all conditions of the system. For instance, the desired P and I coefficients in the winter may differ from that of the summer, or they may vary during the time by the aging of the equipment. Therefore, an auto-tuned PI-controller as proposed in this paper must be adopted to guarantee the proper performance of the compensator.

In the next section, the proposed HPQC has been designed and simulated, and the simulation results have been investigated, which support the early hypothesis suggested in this paper.

5 Designing HPQC and simulation results

In this section, a typical case study is selected for electric railway, in which the 230 kV transmission line is supposed as the infinite bus. The TSS usually is fed through 230 or 132 kV transmission line, (also, in case of outlying railway lines, it may be fed through 63

kV). The railway power supply system is modelled in [14], in which the system parameters have been calculated as an example. In this paper, the 230/27.5 kV TSS is studied for simplicity, because the HPQC is installed in the secondary side of TSS, and performance of the compensator is independent of the primary side voltage. The parameters of the selected system are shown in Table 1.

For the given system, the SVC can be designed from (1) and (2). The inductors and capacitors of the SVC must be designed for the worst-case that is when the full load is drawn from only one section. Therefore, using (1), the compensation susceptances can be obtained, which is $\pm 4.6 \text{ } \Omega$. To achieve $+4.6 \text{ } \Omega$, the fixed capacitor must be sized at least 14.6 mF, and to have $-4.6 \text{ } \Omega$, since the fixed capacitor cannot be disconnected from the circuit, the susceptance of inductor must be designed to be $-9.2 \text{ } \Omega$ to compensate the capacitor's susceptance. Therefore, the inductor must be sized 1.4 mH. Finally, the SVC requires three 1.4 mH inductors, three 14.6 mF capacitors, and six thyristors with 200 A rated current.

Four independent cases are considered for simulation studies in this paper, as shown in Table 2. The variations of loads in two sections are maintained the same for all four cases, which is shown in Table 3. In this section, for each four cases, the featured waveforms relating to each case are plotted, e.g. three-phase currents, DC-link voltage, and currents NSC and PSC.

For case I, as shown in Fig. 7a, the three-phase currents are seriously unbalanced, for which the NSC and PSC of currents are plotted in Fig. 7b.

For case II, the APQC is simulated before GA-optimisation, and the DC-link voltage is shown in Fig. 8a. Then, the GA-optimisation is applied to APQC, in which the population is considered 20. The evolutionary algorithm achieves to the optimum point after 12 generations. The DC-link voltage for GA-designed APQC is shown in Fig. 8b, in which K_I and K_P are 0.24 and 29, respectively, as defined in (14). The DC-link voltage ripples directly influence the total operation of the compensator. Therefore, an optimum design effectively improves the performance of the APQC, and the HPQC in turn. Comparing the DC-link voltages in Figs. 8a and b, the efficiency of the precise design of DC-link voltage controller is demonstrated.

5.1 Reducing the power-electronic switches rating

In case III, the three-phase currents and the compensation currents (i.e. currents flowing to power-electronic switches) are plotted in Figs. 8b and 9a, respectively. As seen in Fig. 9b, the compensation currents exceed 5000 A, for which the power-electronic switches may have extremely high costs, if not impossible. It should be noted that the switches are designed based on the steady-state currents, and over-currents with the duration of less than a half-cycle can be tolerated (e.g. the current at second 0.1 in Fig. 9b achieves 8000 A, but the switches must be designed with rating of 6000 A).

In case IV, the three-phase currents and the compensation currents are shown in Figs. 10a and b, respectively. The current rating of existing insulated-gate bipolar transistors (IGBTs) in free markets achieves 2400 A, and for higher ratings, the prices would increase exponentially. For example, the rated current of ABB 5SNA 2400E170100 IGBT is 2400 A, which can tolerate the surge currents to 20 kA for a half cycle (i.e. 10 ms). The compensation currents of HPQC, as seen in Fig. 10b, does not exceed 2000 A, which can be an acceptable current for this IGBT. The ratings of the power-electronic switches are effectively reduced in the proposed HPQC, as demonstrated in this section.

In order to adapt 5SNA in the supposed system with a single APQC, it requires 18 IGBTs. Since the rated current of this IGBT is 2400 A, three IGBTs are required in parallel to conduct the compensation current, which is 5800 A in this case. Therefore, the simple APQC is not feasible for the case study, since it requires 18 IGBTs, which causes reliability and cooling problems, in addition to very high cost of these extra IGBTs.

5.2 Improving the performance of compensator

The compensator is expected to eliminate the NSC, harmonics, and reactive power, fully, and the performance of the compensator is related to how much it is successful in these functions. To attain a comparative perspective, the NSC index is defined, as in (15), which is calculated for the two cases III and IV. The NSC and PSC are plotted in Figs. 11a and b, for cases III and IV, respectively. Furthermore, the fast Fourier transform (FFT) and total harmonic distortion (THD) are plotted/calculated in the two cases, as shown in Figs. 12a and b.

The thyristor-controlled impedances have a negative effect on the system's harmonic behaviour, because they cut sine-waves at firing angles. Therefore, it may be expected that the proposed HPQC has harmonic compensation problems. However, as confirmed in the simulation results, the harmonic performance of HPQC is improved. This is as a result of the fact that the control unit of the APQC senses the harmonics in the presence of higher currents,

Table 4 Comparison among different design schemes of railway system

	Feature	No compensator	APQC	HPQC
performance	nominal IGBT currents	–	5800 A	2100 A
	surge currents of IGBT	–	8800 A	8600 A
	maximum ripple of DC-link voltage	–	3.4%	<0.5%
	NSC index (min–max)	0.5–1	0.02–0.36	0.07–0.1
structure	THD	13.1%	4.77%	4.63%
	number of IGBTs (ABB 5SNA)	–	18	6
	number of thyristors	–	–	6 ($I_N=200$ A)
	number of capacitors	–	1 × 80 mF	3 × 14.6 mF
	number of inductors	–	–	3 × 1.4 mH

with respect to HPQC. In the HPQC, the control unit senses lower currents with more harmonics, which leads to more harmonic elimination. The THD is calculated 4.77 and 4.63% for APQC and HPQC, respectively. In fact, the harmonic problem of SVC is counteracted by the lack of NSC. In other words, the hysteresis controllers' band-width of HPQC is selected the same as APQC, which leads to a nearly same harmonic performance, with approximate same switching frequency. The DC-link voltage of HPQC is also shown in Fig. 12c, which can be compared with Fig. 7. The DC-link voltage of HPQC is much smoother than its counterpart, because the most important parameter influencing the size of a compensator is the maximum amount of NSC. In Fig. 7, the high ripples in DC-link voltage is a result of the fact that the APQC transfers high amount of active power between phases, due to the high amount of NSC. Besides, for the DC-link voltage, an amount of voltage ripple can be acceptable in converters (i.e. <4%), which provides the option of reducing the DC-link capacitor and its voltage level, to reduce the total cost of the system. Finally, a brief comparison is provided in Table 4, validating the early proposition, which claimed about the effectiveness of the proposed HPQC

$$\text{NSC} \cdot \text{Index} = \frac{\text{NSC}}{\text{PSC}} \quad (15)$$

5.3 Sensitivity analysis to variation of the system parameters

The parameters of the system may vary during the operation of the system in a long-term. For instance, the line and transformer impedances have different values in winter and summer. Moreover, the DC-link capacitance may vary over time due to the ageing of its insulator (if that is not air or vacuum). The desired PI-controller must provide its function to maintain the DC-link voltage for all conditions of the system, and the variation of the system parameters requires the P and I parameters to be able to vary accordingly. Therefore, the auto-tuned PI-controller, as introduced in this paper, tunes the P and I parameters in order to achieve the proper DC-link voltage fixing, since the operation of the compensator is highly influenced by the operation of DC-link operation.

In this part, the performance of the auto-tuned PI-controller is examined for the variation of the DC-link capacitor. The capacitor is supposed to be decreased 5% after a year, from 80 to 76 mF. The DC-link voltages are drawn in Fig. 13 for the constant PI-controller and auto-tuned PI-controller, respectively. As seen in Fig. 13a, the undershoot and overshoot are highly increased because of the decreasing of the DC-link capacitor. However, the auto-tuned PI-controller, as seen in Fig. 13b, demonstrates less sensitivity to the variation of the capacitance. Therefore, the

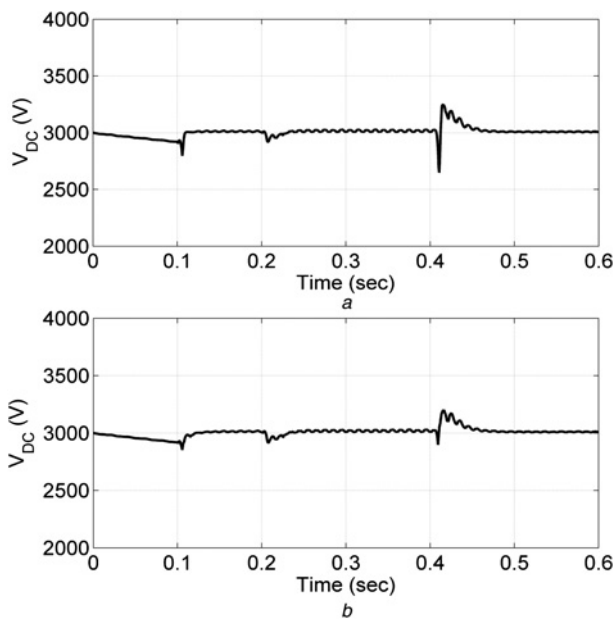


Fig. 13 DC-link voltage for $C = 76 \text{ mF}$

a For the constant PI-controller
b For auto-tuned controller

auto-tuned PI-controller helps the performance of the compensator over time with a low cost, since it can be implemented on a simple processor with a low cost.

6 Conclusion

With the growth of the railway industry, power quality conditioning becomes a necessary part of systems. APQC can be an ideal compensator; however, with increasing the TSS currents it may be impossible to adopt a high-current power-electronic switch. In this case, an alternative compensation scheme is proposed in this paper, in which the NSC current is devolved to SVC, reducing the rating of power-electronic switches, effectively. Simulation studies have been used to try out the efficiency of the proposed method, which support the early hypothesis. Moreover, the performance of the proposed HPQC has been examined, and compared with the APQC. Owing to the proposed HPQC, it is observed that the rating of APQC is reduced advantageously, and the NSC

compensation improves with no negative effect on harmonic currents. Moreover, the DC-link voltage ripples are strongly reduced, which provides the option of reducing the DC-link capacitor, to cut even more costs of the APQC. A brief comparison validates the proposition, which claimed about the effectiveness of the proposed HPQC.

7 Acknowledgments

The authors gratefully thank Dr. Alfred Baghrmian and Dr. Andrea Mariscotti for their valuable helps and supports.

8 References

- 1 Armstrong, A.H.: 'The economic aspects of railway electrification', *J Franklin Inst.*, 1921, **191**, (4), pp. 493–502
- 2 González-Gil, A., Palacin, R., Batty, P., *et al.*: 'A systems approach to reduce urban rail energy consumption', *Energy Convers. Manage.*, 2014, **80**, pp. 509–524
- 3 Chen, T.-H.: 'Comparison of Scott and LeBlanc transformers for supplying unbalanced electric railway demands', *Electr. Power Syst. Res.*, 1994, **28**, (3), pp. 235–240
- 4 Gazafriadi, S.M., Tabakhpour Langerudy, A., Fuchs, E.F., *et al.*: 'Power quality issues in railway electrification: a comprehensive perspective', *IEEE Trans. Ind. Electron.*, 2015, **62**, (5), pp. 3081–3090
- 5 Kazemi, A., Koochi, A.M., Rezaei pour, R.: 'A dynamically SVC based compact control algorithm for load balancing in distribution systems', *Int. J. Energy*, 2007, **1**, (3), pp. 72–76
- 6 Brenna, M., Capasso, A., Falvo, M.C., *et al.*: 'Investigation of resonance phenomena in high speed railway supply systems: theoretical and experimental analysis', *Electr. Power Syst. Res.*, 2011, **81**, (10), pp. 1915–1923
- 7 Sainz, L., Monjo, L., Riera, S., *et al.*: 'Study of the Steinmetz circuit influence on ac traction system resonance', *IEEE Trans. Power Deliv.*, 2012, **27**, (4), pp. 2295–2303
- 8 Morimoto, H., Ando, M., Mochinaga, Y., *et al.*: 'Development of railway static power conditioner used at substation for Shinkansen'. Proc. Power Conversion Conf. 2002. PCC-Osaka, 2002
- 9 Chuanning, W., An, L., Shen, J., *et al.*: 'A negative sequence compensation method based on a two-phase three-wire converter for a high-speed railway traction power supply system', *IEEE Trans. Power Electron.*, 2012, **27**, (2), pp. 706–717
- 10 Zhuo, S., Xinjian, J., Dongqi, Z., *et al.*: 'A novel active power quality compensator topology for electrified railway', *IEEE Trans. Power Electron.*, 2004, **19**, (4), pp. 1036–1042
- 11 Ning-Yi, D., Man-Chung, W., Keng-Weng, L., *et al.*: 'Modelling and control of a railway power conditioner in co-phase traction power system under partial compensation', *IET Power Electron.*, 2014, **7**, (5), pp. 1044–1054
- 12 Wen-Shyan, C., Jyh-Cherng, G.: 'A new hybrid SVC scheme with Scott transformer for balance improvement'. Rail Conf., 2006
- 13 Ghassemi, A., Fazel, S.S., Maghsoud, I., *et al.*: 'Comprehensive study on the power rating of a railway power conditioner using thyristor switched capacitor', *IET Electr. Syst. Transp.*, 2014, **4**, (4), pp. 97–106
- 14 Raygani, S.V., Tahavorgar, A., Fazel, S.S., *et al.*: 'Load flow analysis and future development study for an AC electric railway', *IET Electr. Syst. Transp.*, 2012, **2**, (3), pp. 139–147